

Nonmonotonic Composition Dependence of the Dielectric Response of $\text{Ba}_{1-x}\text{Ca}_x\text{ZrO}_3$

Joseph W. Bennett,* Ilya Grinberg, and Andrew M. Rappe

The Makineni Theoretical Laboratories, Department of Chemistry, University of Pennsylvania, Philadelphia, Pennsylvania 19104-6323

Received April 1, 2008. Revised Manuscript Received May 27, 2008

We use first-principles density functional theory calculations to investigate the dielectric response of BaZrO_3 based perovskites. In this study we have substituted Ca for Ba over a range of compositions to understand what causes the recently reported (Levin et al., *J. Solid State Chem.* **2003**, 175, 170) nonmonotonic dielectric response of $\text{Ba}_{1-x}\text{Ca}_x\text{ZrO}_3$ (BCZ). We show that in all compositions studied there appear two new sets of IR active phonon modes that increase the dielectric constant ϵ . One set occurs below the normal IR active A-O modes, due to the “rolling cation” motion of Ca about its O_{12} cage. The second set of new phonon modes occurs between the normal A-O and B-O mode frequencies, caused by the displacement of Ca along one Cartesian direction. As more Ca is added to BCZ, Ca–Ca interactions increase, leading to Ca displacements in all three Cartesian directions, stronger Ca–O bonds and increased O_6 tilts. Such structural deformations decrease ϵ . These effects are responsible for the anomalous compositional dependence of the BCZ dielectric response.

I. Introduction

Dielectric materials are widely used in wireless communication devices. These require a high dielectric constant, ϵ , and low dielectric loss.¹ Barium zirconate, BaZrO_3 (BZ), is an ABO_3 perovskite dielectric material that is both chemically and mechanically stable. Since dielectric properties are often optimized by varying material composition, there is a need to understand the impact of doping on the local structure and properties of a material. One study showed that the dielectric constant of BZ can be increased by up to 50% by doping with small amount of Ca^{2+} as seen in Figure 1. This is interesting because CaZrO_3 (CZ) has a lower ϵ than BZ. Such a nonlinear dependence of ϵ on composition was also observed in Ba-based perovskites with other B-site compositions.^{3–6} In this paper, we use first principles calculations to study the BCZ solid solution at a variety of compositions, including some that were not accessible experimentally.² We show how the changes in static struc-

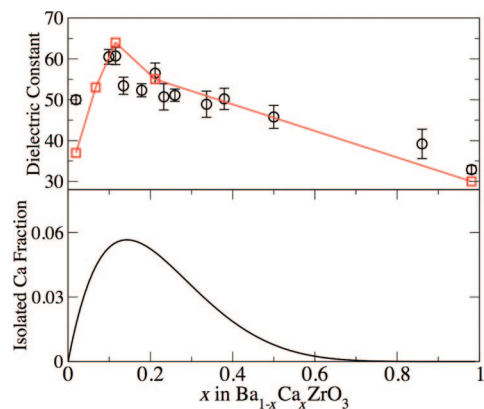


Figure 1. Directionally averaged ($T = 0$ K) dielectric constant ϵ vs Ca content x in BCZ. The ϵ values are also averaged over cation orderings. Black circles are the averaged diagonal elements of the ϵ tensor. Low T experimental values⁶ are shown as red squares. Also shown is the fraction of isolated Ca atoms, $x(1-x)$, as a function of x .

tural features influence the dynamical behavior of these materials, giving rise to a new vibrational mechanism and enhanced dielectric response.

II. Methodology

In this study, two first-principles codes are used. An in-house solid state DFT code, BH, used in previous studies^{7,8} and the

- (1) Fortin, W.; Kugel, G. E.; Grigas, J.; Kania, A. *J. Appl. Phys.* **1996**, 79, 4273.
- (2) Levin, I.; Amos, T. G.; Bell, S. M.; Farber, L.; Vanderah, T. A.; Roth, R. S.; Toby, B. H. *J. Solid State Chem.* **2003**, 175, 170.
- (3) Ikawa, H.; Touma, M.; Shirakimi, T.; Fukunaga, O. In *Electroceraamics IV*; Waser, R., Hoffman, S., Bonnenzberg, D., Hoffman, C., Eds.; Verlag der Augustinus Buchhandlung: Aachen, 1994; pp 41–46.
- (4) Ikawa, H.; Yashamiro, M.; Niwa, T.; Omata, T.; Takemoto, M. In *Electroceraamics V*; Baptista, J. L., Labrincha, L. A., Vilarinho, P. M., Eds.; University of Aveiro: Aveiro, 1996; pp 41–44.
- (5) Ikawa, H.; Takemoto, M. *Mater. Chem. Phys.* **2003**, 79, 222.
- (6) Ikawa, H.; Takemoto, M.; Katouno, M.; Takamura, M. *J. Eur. Ceram. Soc.* **2003**, 23, 2511.
- (7) Grinberg, I.; Cooper, V. R.; Rappe, A. M. *Phys. Rev. B* **2004**, 69, 144118.

- (8) Mason, S. E.; Grinberg, I.; Rappe, A. M. *Phys. Rev. B* **2004**, 69, 161401(R).

ABINIT software package⁹ are used to relax the ionic positions and lattice constants. The local density approximation (LDA) of the exchange correlation functional and a $4 \times 4 \times 4$ Monkhorst–Pack sampling of the Brillouin zone¹⁰ are used for all calculations. All atoms are represented by norm-conserving optimized¹¹ designed nonlocal¹² pseudopotentials. All pseudopotentials are generated using the OPIUM code.¹³ The calculations are performed with a plane wave cutoff of 50 Ry.

At low temperatures, the ground-state structure of BZ is an irreducible $2 \times 2 \times 2$ pseudocubic unit cell,¹⁴ containing O_6 tilt angles that range between 3.6 and 4.2° . The computed BZ ϵ is 50 (45 from the ionic contribution and 5 from the electronic) at 0 K, larger than the value reported at room temperature. This is caused by the frozen tilts present at low T . Approximating the ground-state BZ by a 5-atom cell¹⁵ leads to a significant overestimation¹⁴ of ϵ at $T = 0$. Therefore, the majority of the calculations in our study were performed on $2 \times 2 \times 2$ supercells of BCZ. The ground-state structure of CZ at low temperatures is orthorhombic, displaying O_6 tilt angles that vary between 17.1 and 17.5° . The computed CZ ϵ is 30, about half that of BZ. In the ground-state CZ structure, antiferroelectric displacements of Ca atoms are mostly along one Cartesian direction, with an average magnitude of 0.4 \AA . This is over an order of magnitude larger than the displacements of Ba seen in BZ. We also performed calculations for $3 \times 3 \times 1$ supercells. In these cases, Ca was substituted for Ba at $x = 1/9$, $x = 2/9$, and $x = 1/3$. For $1 \times 1 \times n$ and $2 \times 1 \times n$ supercells, where n was varied from 2 to 6, $x = 1/n$ and $x = 2/n$ are considered. This was performed in order to see the effects of Ca substitution on nearest neighbor unit cells. Several different sets of initial ionic coordinates were used in the relaxations for each composition to ensure that the complicated potential energy surface of the material was adequately explored. For all compositions, we found that the DFT-LDA optimized lattice constants were within 1.5% of the experimental values.

After a structure was fully relaxed, response function^{16,17} calculations were performed using ABINIT to generate the mass-weighted dynamical matrix which was then used to calculate the directionally averaged dielectric constant ϵ at $\Gamma = 0$. Contributions to ϵ come only from IR active Γ point phonon modes.¹⁸ Details of this method are presented in a previous study.¹⁴ A full listing of the diagonal elements of the ϵ tensor is provided in the Supporting Information, Tables I and II. A comparison of the experimental and computed ϵ for the entire compositional range of BCZ is presented in Figure 1. The magnitude of the experimental² and theoretical dielectric constants show reasonable agreement, with both showing the trend of an initial sharp increase up to 10% Ca and subsequent gradual decrease in ϵ with greater Ca fraction.

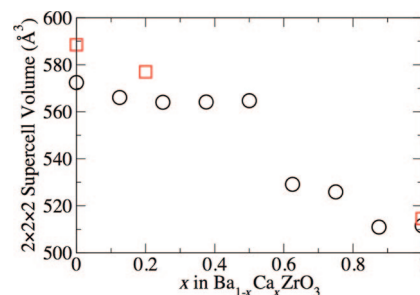


Figure 2. BCZ cell volume changes as Ca is added. The volume does not monotonically decrease but plateaus until Ca is the majority A-site cation. Squares are experimental values² and circles are DFT-LDA from the present study.

III. Results

The unit cell volume is the most basic characteristic of the solid-state structure. The volume of BZ is 16% larger than that of CZ, and one might expect a simple linear change in the volume as Ca fraction is increased. Somewhat surprisingly, we find that as Ca is added to BZ, the volume of BCZ does not monotonically decrease (Figure 2). In compositions $x = 0$ through $x = 0.50$ for $2 \times 2 \times 2$ supercells, the volume remains nearly constant. Then, when Ca becomes the majority A-site, the volume drastically decreases. This is supported by the change in volume from components to solid solution for $x = 0.125$ through $x = 0.50$ and then subsequent decrease at $x = 0.875$. A trend that is different from this is the near monotonic increase in formation energy for these supercells. Both are presented in the Supporting Information. Comparison of our results with available experimental data shows close agreement between DFT and experimental lattice constants. The relaxed volumes are slightly underestimated by DFT-LDA, as expected. The constant volume for $x < 0.50$ implies that the changes in ϵ for these compositions are not due to volume effects; rather they are caused solely by the changes in structural distortions at the same volume.

Several important structural changes are induced by Ca doping into BZ. While the Ba atom in BZ is located at the high-symmetry position in the center of the O_{12} cage, Ca atoms in BCZ displace significantly toward a low-symmetry position. The small Ca forms shorter Ca–O bonds along (110), to satisfy bonding requirements, by displacing in (100). Ca displacements increase with increased Ca doping, from 0.3 \AA at $x = 0.125$ to 0.5 \AA at $x = 0.5$. This is somewhat larger than the 0.4 \AA displacements of Ca in CZ and is due to the larger volume of BCZ.

The direction of Ca displacements shows a dependence on Ca concentration. At low doping levels, Ca displacements are parallel to each other along (100). As more Ca is added, Ca–Ca interactions increase and O_6 octahedra rotate to accommodate the displaced Ca. This locally reduces the available volume and gives rise to Ca displacement components in other directions, such as (110). The total magnitude of Ca displacement continues to increase with increasing x , although the displacement component along the (100) direction is nearly unchanged. Such distortions are also seen in CZ. Thus, as the Ca fraction rises, the Ca local environ-

(9) Gonze, X.; Beuken, J.-M.; Caracas, R.; Detraux, F.; Fuchs, M.; Rignanese, G.-M.; Sindic, L.; Verstraete, M.; Zerah, G.; Jollet, F. *Comput. Mater. Sci.* **2002**, *25*, 478.

(10) Monkhorst, H. J.; Pack, J. D. *Phys. Rev. B* **1976**, *13*, 5188.

(11) Rappe, A. M.; Rabe, K. M.; Kaxiras, E.; Joannopoulos, J. D. *Phys. Rev. B: Rapid Commun.* **1990**, *41*, 1227.

(12) Ramer, N. J.; Rappe, A. M. *Phys. Rev. B* **1999**, *59*, 12471.

(13) <http://opium.sourceforge.net>.

(14) Bennett, J. W.; Grinberg, I.; Rappe, A. M. *Phys. Rev. B* **2006**, *73*, 180102(R).

(15) Akbarzadeh, A. R.; Kornev, I.; Malibert, C.; Bellaiche, L.; Kiat, J. M. *Phys. Rev. B* **2005**, *72*, 205104.

(16) Gonze, X.; Lee, C. *Phys. Rev. B* **1997**, *55*, 10355.

(17) Ghosez, P.; Michenaud, J.-P.; Gonze, X. *Phys. Rev. B* **1998**, *58*, 6224.

(18) Cockayne, E. J. *Eur. Ceram. Soc.* **2003**, *23*, 2375.

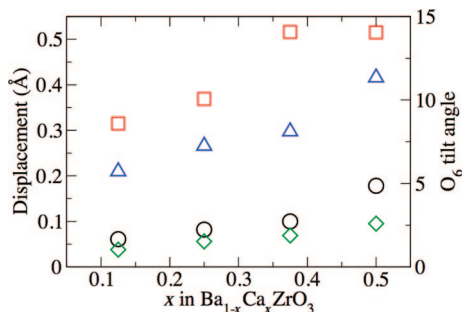


Figure 3. Cation displacements for $x = 0.125, 0.250, 0.375,$ and 0.500 . Average displacement increases with the addition of Ca. Ba is shown as circles, Ca is shown as squares, and Zr is shown as diamonds. Average O_6 tilt angle (in degrees) increases with the addition of Ca, shown here as triangles.

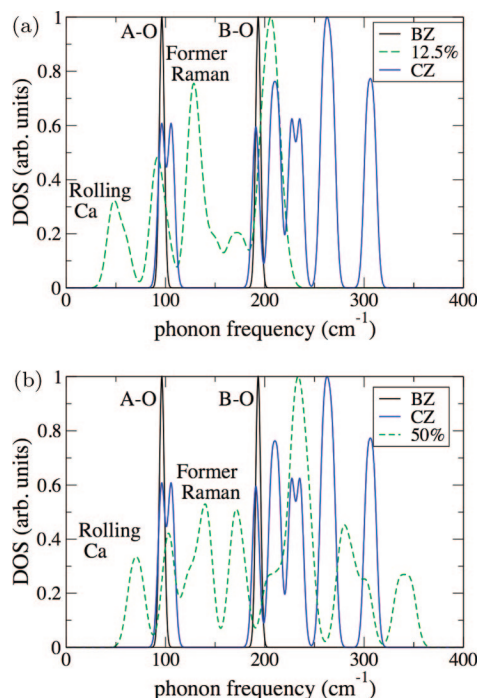


Figure 4. IR active phonon frequency comparisons of $2 \times 2 \times 2$ BCZ to BZ, shown in black, and CZ, shown in blue. Not shown are O_6 modes above 400 cm^{-1} , which do not shift as significantly. (a) $\text{Ba}_{0.875}\text{Ca}_{0.125}\text{ZrO}_3$. (b) $\text{Ba}_{0.50}\text{Ca}_{0.50}\text{ZrO}_3$. All show IR active low frequency phonon modes that are not present in either BZ or CZ, as well as more modes centered around 130 cm^{-1} .

ment and distortions become more similar to those observed in the CZ end member.

The presence of Ca displacements induces Ba and Zr atoms to displace as well, opposing the Ca. These displacements are small ($\approx 0.1 \text{ \AA}$) and are localized on the Ba and Zr atoms adjacent to Ca. The structural trends are shown in Figure 3. Finally, the presence of small Ca atoms increases the average O_6 tilt angle in BCZ with increasing x .

The changes in the structural properties described above give rise to a new dielectric response mechanism and increased value of ϵ . In BZ, ϵ is 50. In BCZ compositions below $x = 0.15$, computed ϵ is as high as 70. The breaking of symmetry induced by $x = 0.125$ Ca doping broadens the discrete Γ point phonon frequencies of BZ into a distribution of frequencies, as shown in Figure 4. Most importantly, new IR active phonon modes appear at frequencies that are not

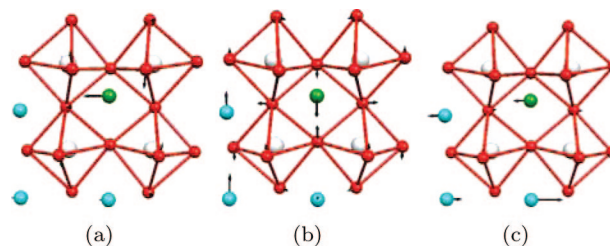


Figure 5. IR active phonon modes in $\text{Ba}_{0.875}\text{Ca}_{0.125}\text{ZrO}_3$. Ba atom is shown as blue, Ca is green, Zr is white, and O is red. Arrows depict relative atomic displacements. (a) The rolling cation motion associated with Ca. This mode occurs at 49 cm^{-1} , below (b) at 60 cm^{-1} where Ca moves along the direction of its displacement from high symmetry. (c) All A-sites move, which occurs at 93 cm^{-1} .

present in BZ. In the parent BaZrO_3 material, three sets of IR active modes contribute to ϵ . The lowest-frequency set of phonon modes, occurring around 100 cm^{-1} and contributing the most to the dielectric constant, is of the Last type and consists of Ba rattling inside its O_{12} cage. Similarly, in CZ, the Ca–O modes at $96, 106,$ and 191 cm^{-1} are lowest in frequency, making a large contribution to ϵ . In BCZ, at low x , the introduction of Ca leads to the appearance of three very low frequency modes at $40 \text{ cm}^{-1}, 49 \text{ cm}^{-1},$ and 60 cm^{-1} . Since ϵ is proportional to $1/\omega^2$, the presence of such low frequency modes significantly enhances the dielectric constant. The increased number of Ca atoms gives rise to a greater intensity of the low-frequency modes and leads to an initial increase in the dielectric constant with Ca content.

Examination of the eigenvector for the new low-frequency vibrations reveals both similarities and differences between these modes and the Ca–O vibrational modes found in CZ. The atomic motions are mainly Ca–O into which some Ba–O motion is mixed, as shown in Figure 5a. Thus, the modes induced by the Ca doping are localized around the Ca sites. This is unlike the Last type phonon modes in both BZ and CZ, where all A-site displacements are similar in magnitude (Figure 5(c)). However, the motion of the Ca in its cage is similar to that found in CZ. For example, in $x = 0.125$ composition, Ca displaces toward one O along the (001) axis forming a stronger Ca–O bond in the direction of displacement. This leaves elongated Ca–O bonds in the other two Cartesian directions. The weakened bonds lead to a low frequency of Ca oscillations perpendicular to the Ca displacement, giving rise to two low frequency modes at 45 cm^{-1} and 49 cm^{-1} . Ca oscillation in the direction of Ca off-center displacement (shown in Figure 5b) has a higher mode frequency (60 cm^{-1}), suggesting a stronger bond. Similar eigenvectors are found for the Ca–O modes in the end-member of CZ, however at significantly higher frequencies ($96 \text{ cm}^{-1}, 106 \text{ cm}^{-1},$ and 191 cm^{-1}). The lower frequencies of Ca–O oscillations in BCZ are due to the large volume of the Ca– O_{12} cage, making the Ca–O bonds weaker. Bond-valence sums support our DFT finding of weaker Ca–O bonds in BCZ. We find that Ca bond valence computed using relaxed DFT structures is 1.8 for Ca in BCZ and 2.05 for Ca in CZ. Similar conclusions about the weak bonding for Ca in BCZ were reached by Levin et al. using bond valence analysis of structures obtained from refinement of neutron diffraction data.²

The Ca motions in CZ and BCZ differ from the common rattling cation model of ionic vibrations in perovskites. In this model, it is assumed that the ionic vibrations are due to the oscillations of a cation from its central location within the unit cell and are similar in all three Cartesian directions. This is the case for Ba in BZ¹⁴ and for the Ba atoms in BCZ. However, in BCZ the oscillation of the Ca around its off-center, low-symmetry position is noticeably more pronounced in the two Cartesian directions perpendicular to the direction of Ca off-center displacement. This gives rise to an arc-like motion similar to that of a hindered rotor, with the Ca atom rolling on the surface of a sphere. The energy required to excite such a “rolling cation” motion in BCZ is less than that for the usual rattling cation mode, leading to a strong enhancement of the A-site dielectric response.

The introduction of Ca into BZ also transforms some of the modes that are Raman active in BZ into IR active modes in BCZ. This is caused by local dipoles created by Ca displacement. These modes occur around the frequency of the strongest Ca–O mode in CZ and are localized on Ca and its surrounding ions. At low doping levels, the local environment of displaced Ca in BCZ is similar to that of displaced Ca in CZ, so phonon modes at these frequencies are similar. However, as more Ca is added to BCZ, it causes the surrounding O_6 octahedra to increase their tilt angles to accommodate increased Ca displacement. This increased tilting causes not only Ba to displace but Zr as well, creating displacements which are further enhanced by an induced phonon mode. These modes are fairly high in frequency and therefore provide only a small increase in the dielectric response.

We now discuss the compositional dependence of the dielectric constant in BCZ. Figure 4a,b shows that as Ca content increases past $x = 0.125$, the A–O and B–O BZ-derived modes are further broadened over a wider range of frequency. The O_6 modes and electronic contributions, not shown, display the least compositional dependence. The total directionally averaged B–O contribution to the dielectric constant is in the range of 18–20, and the O_6 and electronic contributions are both ≈ 5 for all compositions. The largest changes are observed for Ca–O rolling cation modes, where an increase in x causes stronger Ca–O bonds in all three Cartesian directions. This manifests as an increase in the phonon frequencies associated with these modes. Although at $x = 0.25$ the intensity of the low-frequency Ca–O modes is larger than at $x = 0.125$, their contribution to the dielectric constant is smaller due to the blueshift in the Ca–O mode frequencies and the $1/\omega^2$ dependence of the dielectric constant. This leads to a decreased dielectric constant at $x = 0.25$ relative to $x = 0.125$. Further increase in Ca concentration introduces more Ca–Ca interactions and gives rise to further upshift of the Ca–O modes. Similar to the Ca–O modes, the frequency of the former Raman modes shifts up with increased Ca concentration so that the contribution to ϵ due to the former Raman modes first increases (at low x_{Ca}) and then decreases (for higher x_{Ca}) with increasing Ca content. For $x > 0.5$, the phonon modes become less broad and there is a general shift to higher ω values, further decreasing the dielectric response.

The nonmonotonic dielectric constant dependence on composition is due to the local structural changes resulting from increased Ca content. For small Ca concentrations, the localized character of the low frequency modes means that Ca–Ca interactions will have a small impact on the Ca–O vibrational frequencies. This leads to a linear increase in the intensity of the low-frequency Ca modes and therefore ϵ as the number of Ca is increased.

The decrease of the dielectric constant with increasing Ca content is due to the structural changes induced by the presence of two Ca atoms in close proximity to one another, found frequently for nondilute solid solution compositions. The first Ca that is added to a BZ supercell displaces along (100). In 40-atom supercells with two Ca atoms ($x = 0.25$), Ca atoms coordinate their displacements mostly in (100), but with some components in (110) and (101). This is because the large O_6 tilts induced by the close proximity of two Ca atoms limits the available volume. At low doping levels, Ca displace parallel to each other along (100), but at higher doping levels, structural deformations limit their ability to do so. This effect becomes stronger with additional Ca, until large directional displacements are no longer feasible and smaller displacements are made along (111). Total Ca displacements increase, but the components in each direction are smaller than at lower dopant values. Off-center displacements in the directions perpendicular to the primary distortion direction strengthen the Ca–O bonds, increasing the Ca–O frequency and decreasing ϵ .

The dielectric constant peaks at compositions for which Ca–Ca interactions are not strong. This suggests that the turnover should take place at x for which the population of Ca atoms with at least one Ca nearest neighbor is rising rapidly with composition. Simple statistics show that such a rise is present at small x ($x < 0.15$) in BCZ, with the probability of Ca atom surrounded by only Ba nearest neighbors reaching its maximum value at $x = 0.14$, as shown in Figure 1. At this x , the maximum amount of Ca having no nearest Ca neighbors is 6%. This explains why the turnover in ϵ of BCZ occurs at low x , as observed experimentally and in our DFT calculations. For low x , Ca–Ca interactions are rare and do not hinder the “rolling cation” motion. As x increases, nearest Ca–Ca neighbors become predominant, causing a decrease in the “rolling cation” motion. The mechanisms described above do not depend on the particular chemistry of Ba, Ca, and Zr ions but are due to a size mismatch on the perovskite A-site between the majority Ba cation and the minority Ca cations. Therefore we expect that the effects discussed above are relevant whenever doping a large cation perovskite A-site with a smaller cation.

IV. Conclusions

We performed a study of the nonmonotonic dielectric properties of the BCZ solid solution using first-principles calculations. We find that addition of Ca to BZ gives rise to two new sets of phonon modes. The first set are low frequency Ca–O modes that occur at frequencies below either Ca–O or Ba–O in their native structures. Their contribution to ϵ varied according to local structure. The

second set of frequencies were Raman active modes that had become IR active with the introduction of Ca. The presence of very low frequency Ca–O modes initially increases the dielectric constant of the material. The much lower frequencies of Ca–O vibrations in BCZ relative to CZ are due to placing Ca into a large O_{12} cage, giving rise to weak Ca–O bonds. Due to the large Ca displacement in its O_{12} cage, Ca oscillations are asymmetric and can be described by the “rolling cation” model, with Ca rolling on the surface of a sphere. At higher Ca content, Ca–Ca interactions lead to a blueshift of the Ca–O modes and a decrease of the dielectric constant. The effects described for BCZ should be general to all dielectric perovskite systems in which a smaller A-site

cation has been substituted into a larger A-site perovskite for a range of compositions.

Acknowledgment. This work was supported by the DOE, DE-FG02-07ER46431, ONR, N00014-00-1-0372, and an NSF MRSEC grant, DMR05-20020. Computational support was provided by DoD HPCMO.

Supporting Information Available: Formation energies, volumes of formation, and data for $2 \times 2 \times 2$ and $1 \times 1 \times n$, $2 \times 1 \times n$, and $3 \times 3 \times 1$ supercells (PDF). This material is available free of charge via the Internet at <http://pubs.acs.org>.

CM800929E